Materials Research. 2015; 18(3): 468-472
DOI: http://dx.doi.org/10.1590/1516-1439.298014

On the Formation of Hydroxyapatite Nano Crystals Prepared Using Cationic Surfactant

***Mohammad Mujahid*[a]*, Sadaf Sarfraz[b], Shahid Amin[c]**

[a]*School of Chemical and Materials Engineering, National University of Sciences and Technology, Sector H-12, Islamabad, Pakistan*
[b]*Lahore College for Women University, Jail Road, Lahore-54000, Pakistan*
[c]*PINSTECH, PO Box 1356, Islamabad, Pakistan*

Received: May 26, 2014; Revised: May 17, 2015

Being a major constituent of hard tissues found in humans, synthetic hydroxyapatite (HA) as a substitute to natural bone and teeth is gaining importance. In particular, nano hydroxyapatite is expected to impart considerably superior properties. The current research focuses on identification of mechanism of the formation of HA nano-crystals during its preparation when surfactant nano reactors are used for their nucleation and growth. In addition to having a rod-shaped morphology, high resolution electron microscopy has revealed the presence of 2-5 nm crystals within individual particles of HA. The HA particles were not completely hollow, rather nano sized spherical pores of about 5 nm size, have been observed in TEM. These pores are suggested to have formed due to evolution of gases during processing.

Keywords: *biomaterials, hydroxyapatite, synthesis, nanomaterials, HRTEM, nano-crystalline*

1. Introduction

Development of synthetic replacement materials for orthopedic and orthodontic applications has been the subject of active research. Traditionally, the key ingredient of hard tissues in humans is a calcium phosphate, called hydroxyapatite (HA) or $Ca_5(PO_4)_3OH$[1]. Besides this, the remaining constituents are living cells and collagenous matrix. As a bone graft substitute, the synthetic materials are expected to assist and encourage natural cell growth and extracellular matrix formation[2-4]. Other important calcium phosphate phases, such as α and β tri-calcium phosphates, have also been used in bioresorbable applications[4].

Although synthetic HA is exceptionally biocompatible, its use has been limited to non load-bearing applications. This is because of its inadequate mechanical properties, resulting from poor compaction and sintering characteristics[5]. It is believed that nano structured calcium phosphate ceramics can improve the sintering kinetics due to the presence of large surface area and subsequently lead to significant improvement in mechanical properties. In addition, the properties of HA, including bioactivity, solubility, fracture toughness and absorption, can be tailored over wide ranges by controlling the composition, size and morphology of the powder particles[6-8]. For these reasons, it is important to further develop synthesis methods for HA.

Recently, surfactant based systems are being explored for the synthesis of nano-sized materials as they presumably provide very efficient templates for controlling reactions and thus the particle size and shape[9]. The control on the particle size and morphology using molecule-templates has been discussed in many review articles[10-13]. Micelle formation of a surfactant in solution is induced by the hydrophobic interactions between hydrocarbon parts of the surfactant molecules balanced by their hydration and electrostatic repulsive effects[14]. These organized organic surfaces can control the nucleation of inorganic materials by geometric, electrostatic and stereo-chemical complementarities between the embryonic nuclei and the functionalized substrates[15-18]. Surfactant assembly also shows more versatility because the size range of the reaction environment is more extensive and there is potential for molecular engineering of surface functional groups[19]. Cationic surfactants, besides their surface activity, do show some antibacterial properties and are also used as cationic softeners, lubricants, retarding and antiseptic agents and in some cases for consumer uses[20]. Cationic surfactants are well known compounds belonging to quaternary salts and have been examined for their surface solution behavior using variety of methods[21-24].

The present study is focused on preparation of HA nano powder by using surfactant molecular self-assembling technology. A cationic surfactant is used as regulator of nucleation and crystal growth. The formation of hydroxyapatite nano crystals has been investigated by using high resolution electron microscopy.

2. Methods and Material

Hydroxyapatite nano powders were synthesized in nano reactors that are formed when a suitable surfactant is used in the precursor solutions. In the present study, cetyl trimethyle ammonium bromide (CTAB) was used as a surfactant. Other materials used are calcium chloride ($CaCl_2$) and di-potassium hydrogen phosphate (K_2HPO_4). Sodium hydroxide (NaOH) was used to maintain pH of the solution at required levels. All the chemicals were of analytical grade supplied by Merck. Aqueous solutions were prepared by dissolving the chemicals in distilled and de-ionized water.

*e-mail: mujahids@gmail.com

Flow diagram of the synthesis process is shown in Figure 1. In brief, aqueous solutions of calcium chloride and di-potassium hydrogen phosphate were prepared by dissolving the required amounts in 60 ml and 100 ml of de-ionized water respectively. Surfactant solution with a concentration of 0.4 M was prepared by dissolving the required amount of CTAB in 100 ml of de-ionized water. Both the surfactant and phosphate solutions were then mixed together while the pH of the resulting mixture was adjusted to 13 with NaOH. The above solution was kept for two hours to ensure the co-operative interaction and self assembly process of micellization to be completed.

Subsequently the $CaCl_2$ solution was slowly added to the prepared solution mixture, yielding a milky suspension, which was refluxed at 120 °C for 24 h. The precipitates were than filtered and washed with de-ionized water. A gel like paste was produced that was dried in an oven at 100 °C for 24 h. The dried powder was subsequently calcinated in air in a furnace at 550 °C for 5 h to yield HA powder.

To study the composition and functional groups present in the product powder, Fourier transform infrared (FTIR) spectroscopic measurements were taken on Perkin-Elmer FTIR (model Midac 1000 series) spectrophotometer. Infrared spectra were recorded in the region of 500 cm^{-1} to 4500 cm^{-1} with a resolution of 16 cm^{-1}.

The X-ray diffraction (XRD) measurements were taken by using a Bruker D8 Discover powder diffractometer using Cu-K_α radiation with a wavelength of 1.54 Å. The instrument was operated at 40 kV with a current of 40 mA. The specimens were scanned between 2θ range of 15° to 70° at a scanning speed of 4°/min.

The nano powders were characterized including their particle size, shape and morphology by using a Jeol JSM 6340F field-emission scanning electron microscope. Thorough analysis of the crystallite size and shape within individual particles was carried out by using a JEOL 2100 transmission electron microscope also equipped with a field emission gun.

3. Results and Discussion

In order to create nano-reactors of micelles, surfactant is dissolved in water. When cationic surfactants are added to aqueous media, their molecules spread on the surface, resulting in a decrease in surface tension. With increasing concentration of the surfactant, the aqueous surface eventually gets saturated, thereby, encouraging formation of micelles inside the aqueous medium. Depending on the actual concentration of the surfactant above critical micelle concentration (CMC), micelles can have shapes which are either spherical, rods (with varying aspect ratios), or lamellar.

Next, the surfactant solution containing micelles is mixed with the phosphate precursor solution. Adsorption of phosphate onto the micelle surfaces during the surface treatment of micelles occurs due to electrostatic force of attractions of the oppositely charged ions. Subsequently, with the addition of calcium precursor solution, Ca^{2+} approaches the surface of micelles containing phosphate to form calcium phosphate as surface layer (see Figure 2). By adjusting to the required pH, temperature and reflux conditions, the conversion of calcium phosphate to hydroxyapatite took place. These parameters are also important to control the morphology of the nano particles[25]. Significantly high concentration of the surfactant, above the CMC, renders the surfactant molecules to adopt a cylindrical shape. Since the HA particles form on the surface of micelles, they are anticipated to also take a cylindrical shape with an inner core of surfactant molecules. Calcination process is used to eliminate the nano-reactor templates from inside the particles, presumably leaving hollow HA particles, while simultaneously improving crystallinity of HA phase.

The HA powder obtained was observed to have a white color with good flow properties. In powder form, the nano particles of HA are clustered into large agglomerates of irregular shapes. However, the particles are weakly bonded and the clusters break easily with ultrasonic agitation in an aqueous medium. This method was used to prepare samples for SEM and TEM studies. XRD results (Figure 3) revealed the presence of hydroxyapatite phase with a hexagonal crystal structure (PDF card number 009-0432 and 01-072-1243). The crystallite size was calculated by using Scherrer formula[26]. The HA nano particles were composed of tiny crystals of about 5 nm size.

Figure 4 shows FTIR spectrum of the HA after calcination. The bands at 566 cm^{-1} and 607 cm^{-1} are derived from ν_4

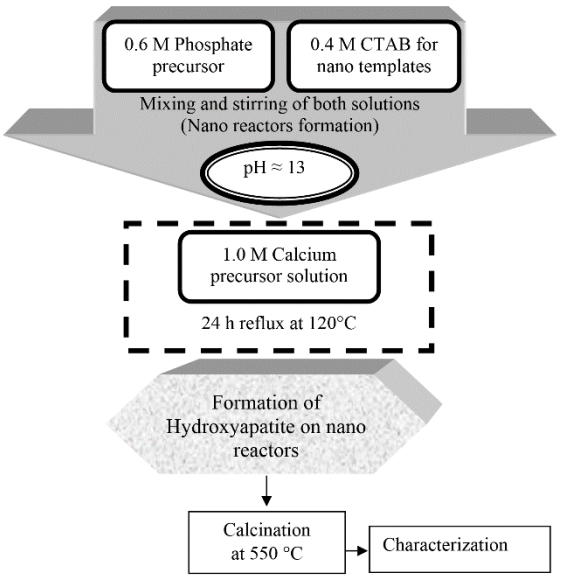

Figure 1. Flow diagram of procedure for the synthesis of nano hydroxyapatite.

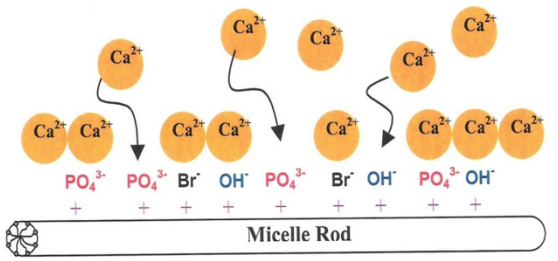

Figure 2. Schematic of hydroxyapatite phase formation on CTAB micelles.

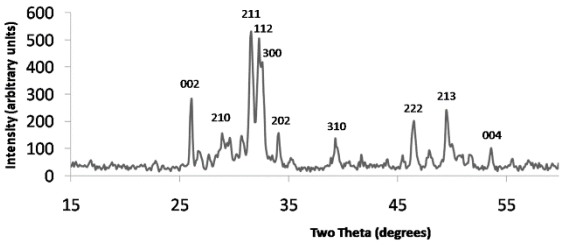

Figure 3. X-ray diffraction pattern of calcined hydroxyapatite powder. All the peaks match with the hexagonal hydroxyapatite.

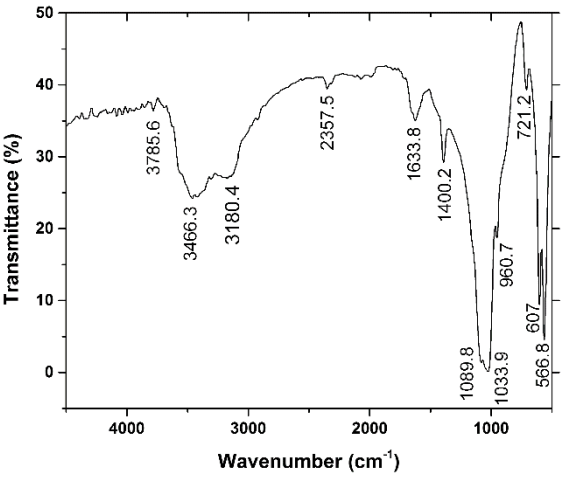

Figure 4. FTIR spectrum of calcined hydroxyapatite.

bending vibrations of P-O mode and the 960 cm^{-1} band resulted from the ν_1 symmetric P-O stretching vibrations[27]. The peaks from 1400 cm^{-1} to 1600 cm^{-1} are attributed to carbonates which are observed in the given spectrum. The strong bands at 1033 cm^{-1} and 1089 cm^{-1} are also assigned to the P – O stretching vibrations of PO_4^{3-}[28]. The broad bands at 3100 cm^{-1} and 3400 cm^{-1} are related to the absorbed water and OH^{-1}, respectively, while the weak peak at 3785 cm^{-1} corresponds to the stretching vibration of OH^{-1} ions in the HA lattice[29]. A very small peak at 2357 cm^{-1} indicates the possible presence of traces of CTAB molecules left in the HA powder after calcination process.

SEM image (Figure 5) shows that the HA powders, as expected, are composed of rod-shaped particles with fairly consistent size and shape distribution – rods having a diameter of about 50 nm and lengths varying between 200-300 nm. There has been no evidence of hollowness or continuous empty space inside the cylindrical particles.

The TEM analysis in Figure 6 shows general shape and distribution of size range of the HA particles, whereas the image of individual particle taken at higher magnification is shown in Figure 7. Complete surface morphology of the cylindrical particles has been revealed. Apparently, individual particles do not have a smooth surface, rather a jagged and very uneven surface is observed. It also shows round bright patches, of size 5 nm or less, distributed randomly in all the particles. These patches are suggested to be nano-pores that may have been formed while the powder is being dried and subsequently calcinated during the final stages of preparation.

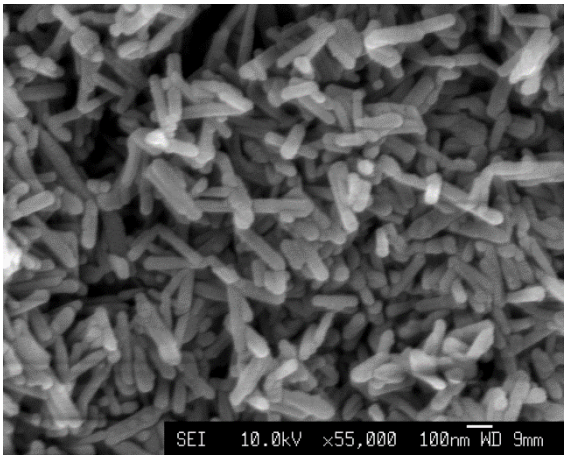

Figure 5. SEM image of rod-shaped nano particles of calcined hydroxyapatite.

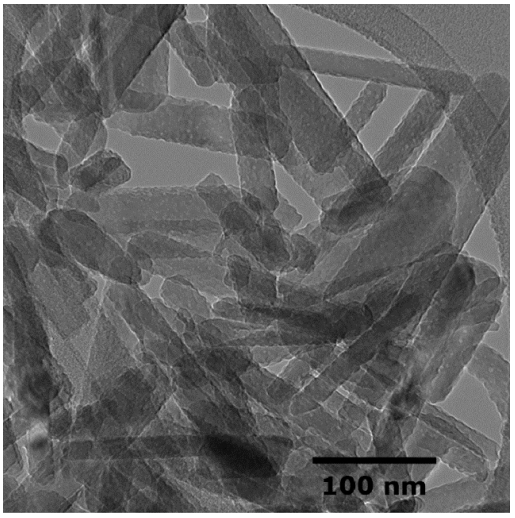

Figure 6. TEM image of nano rods of hydroxyapatite particles showing some variation in size.

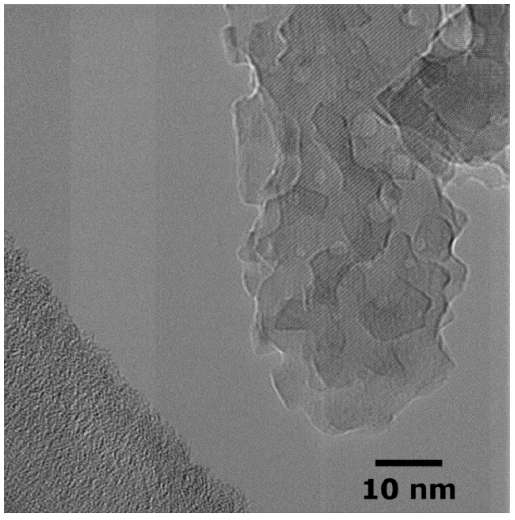

Figure 7. TEM image of a single nano rod of hydroxyapatite showing jagged surface and also spherical nano pores.

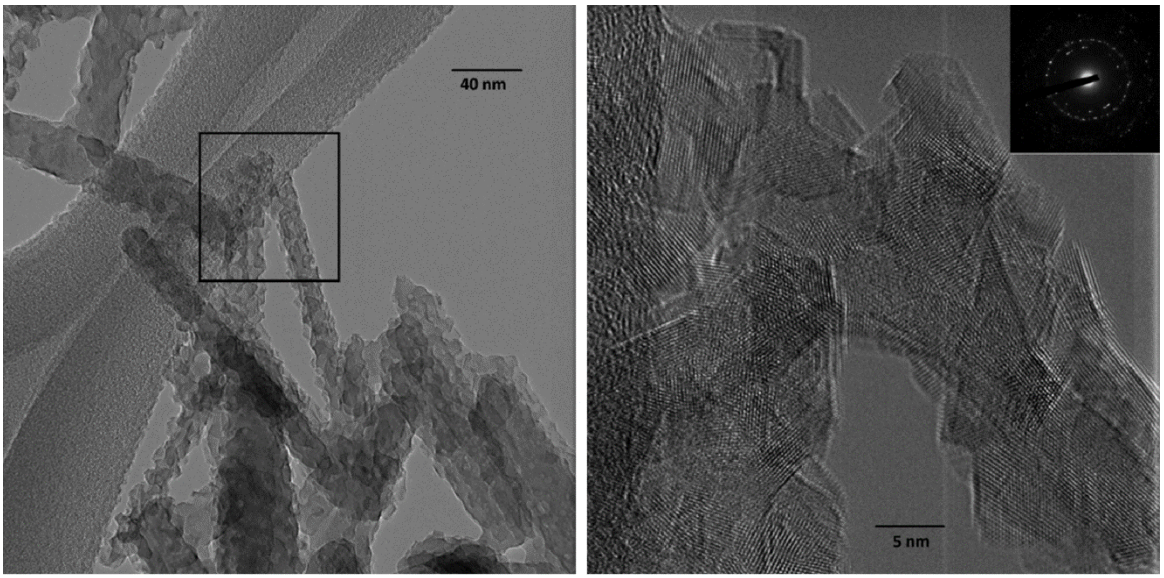

(a) (b)

Figure 8. (a) TEM image showing hydroxyapatite nano rods; (b) electron diffraction and lattice imaging of several nano crystals present in a small part of hydroxyapatite nano rod shown in the square box in (a).

The spherical nature of pores or voids (see Figure 7) is usually attributed to the evolution of gases during processing. It can also be noted here that the particles does not show any evidence of continuous cylindrical porosity throughout the rods. Thus, the particles are not hollow from within as may have been expected due to the proposed mechanism of formation.

It is further revealed by the high-resolution TEM that individual particles are composed of small crystallites. This is evident from Figure 8, where lattice images of many crystallites that form the particle, are revealed clearly and independently. The size of these crystallites is between 3-5 nm. This observation also agrees well with the crystal size calculation according to the XRD. It is proposed that the small crystallites are formed on the surface of the cylindrical-shaped micelles during synthesis. These HA crystals would self assemble to form a continuous film assuming the shape of the micelle, while the surfactant molecules and their hydrocarbon tails are trapped inside forming a core. Calcination of synthesized HA powders would then release the organic surfactant molecules presumably leaving pure, cylindrical shaped HA particles. However, the absence of any large pores or hollowness inside the particles suggest that the self-assembled nanocrystalline film of HA may have collapsed due to the high stresses during calcination, forming a hard solid particle only having small amount of nanopores.

4. Summary

Surfactant nano-reactor technology can be applied to synthesize nano sized hydroxyapatite. The HA nano particles have a rod-shaped morphology with diameters of about 50 nm and lengths of 200-300 nm. The individual HA particles are composed of fine crystallites of 2-5 nm. The nano crystallites of HA self-assemble on the micelle surfaces to replicate the micelle shape. The particles after calcination are not hollow, rather spherical shaped nano pores are observed, which are presumably formed due to evolution of gases during processing.

Acknowledgements

The authors would like to thank the School of Materials Science and Engineering, Nanyang Technological University Singapore for extending their electron microscopy facilities for the present work. Advanced Materials Technologies (AMTech) Islamabad is also acknowledged for their support to the project.

References

1. Léon B and Jansen JA, editors. *Thin calcium phosphate coatings for medical implants*. New York: Springer-Verlag; 2009. http://dx.doi.org/10.1007/978-0-387-77718-4.
2. Burg KJL, Porter S and Kellam JF. Biomaterial developments for bone tissue engineering. *Biomaterials*. 2000; 21(23):2347-2359. http://dx.doi.org/10.1016/S0142-9612(00)00102-2. PMid:11055282.
3. Laurencin CT, Attawia M and Borden MD. Advancements in tissue engineered bone substitutes. *Current Opinion in Orthopaedics*. 1999; 10(6):445-451. http://dx.doi.org/10.1097/00001433-199912000-00005.
4. Zhang P, Hong Z, Yu T, Chen X and Jing X. In vivo mineralization and osteogenesis of nanocomposite scaffold of poly(lactide-co-glycolide) and hydroxyapatite surface-grafted with poly(L-lactide). *Biomaterials*. 2009; 30(1):58-70. http://dx.doi.org/10.1016/j.biomaterials.2008.08.041. PMid:18838160.

5. Tampieri A, Celotti G, Szontagh F and Landi E. Sintering and characterization of HA and TCP bioceramics with control of their strength and phase purity. *Journal of Materials Science. Materials in Medicine*. 1997; 8(1):29-37. http://dx.doi.org/10.1023/A:1018538212328. PMid:15348839.
6. Aaki H. *Science and medical association of hydroxyapatite*. Tokyo: Japanese Association of Apatite Science; 1991.
7. Suchanek WL and Yoshimura M. Preparation of fibrous, porous hydroxyapatite ceramics from hydroxyapatite whiskers. *Journal of the American Ceramic Society*. 1998; 81(3):765-767.
8. LeGeros RZ. *Calcium phosphates in oral biology and medicine*. Switzerland: Karger Basel; 1991.
9. Pileni PM. Nanosized particles made in colloidal assemblies. *Langmuir*. 1997; 13(13):3266-3276. http://dx.doi.org/10.1021/la960319q.
10. Heywood BR and Mann S. Crystal recognition at inorganic-organic interfaces: nucleation and growth of oriented BaSO4 under compressed langmuir monolayers. *Advanced Materials*. 1992; 4(4):278-282. http://dx.doi.org/10.1002/adma.19920040407.
11. Mann S and Ozin GA. Synthesis of inorganic materials with complex form. *Nature*. 1996; 382(6589):313-318. http://dx.doi.org/10.1038/382313a0.
12. Walsh D, Kingston JL, Heywood BR and Mann S. Influence of monosaccharides and related molecules on the morphology of hydroxyapatite. *Journal of Crystal Growth*. 1993; 133(1-2):1-12. http://dx.doi.org/10.1016/0022-0248(93)90097-G.
13. Gray DH, Hu S, Juuang E and Gin DL. Highly ordered polymer-inorganic nanocomposites via monomer self assembly: In situ condensation approach. *Advanced Materials*. 1997; 9(9):731-736. http://dx.doi.org/10.1002/adma.19970090912.
14. Tanford C. *The hydrophobic effect: formation of micelles and biological membranes*. New York: John Wiley; 1980.
15. Mann S, Archibald DD, Didymus JM, Douglas T, Heywood BR, Meldrum FC, et al. Crystallization at Inorganic-organic Interfaces: biominerals and biomimetic synthesis. *Science*. 1993; 261(5126):1286-1292. http://dx.doi.org/10.1126/science.261.5126.1286. PMid:17731856.
16. Mann S. Molecular tectonics in biomineralization and biomimetic materials chemistry. *Nature*. 1993; 365(6446):499-505. http://dx.doi.org/10.1038/365499a0.
17. Archibald DD and Mann S. Template mineralization of self-assembled anisotropic lipid microstructures. *Nature*. 1993; 364(6436):430-433. http://dx.doi.org/10.1038/364430a0.
18. Weissbuch J, Frolow F, Addadi J, Lahav M and Leiserowitz L. Oriented crystallization as a tool for detecting ordered aggregates of water-soluble hydrophobic. alpha.-amino acids at the air-solution interface. *Journal of the American Chemical Society*. 1990; 112(21):7718-7724. http://dx.doi.org/10.1021/ja00177a036.
19. Yan L, Li Y, Deng ZX, Zhuang J and Sun X. Surfactant-assisted hydrothermal synthesis of hydroxyapatite nanorods. *International Journal of Inorganic Materials*. 2001; 3(7):633-637. http://dx.doi.org/10.1016/S1466-6049(01)00164-7.
20. Jungerman E. *Cationic surfactants*. New York: Mercel Dekker; 1969.
21. Ruso JM, Attwood D, Taboada P and Mosquera V. Self-association of n -hexyltrimethyl-ammonium bromide in aqueous electrolyte solution. *Colloid & Polymer Science*. 2002; 280(4):336-341. http://dx.doi.org/10.1007/s00396-001-0610-y.
22. Pal OR, Gaikar VJ, Joshi JV, Goyal PS and Aswal VK. Small-angle neutron scattering studies of mixed cetyl trimethylammonium bromide−butyl benzene sulfonate solutions. *Langmuir*. 2002; 18(18):6764-6768. http://dx.doi.org/10.1021/la0200919.
23. Galán JJ, Gonzáles-Pérez A, Del Cactillo JL and Rodríguez JR. Thermal parameters associated to micellization of dodecylpyridinium bromide and chloride in aqueous solution. *Journal of Thermal Analysis and Calorimetry*. 2002; 70(1):229-234. http://dx.doi.org/10.1023/A:1020678222376.
24. Fujio F, Mitsui T, Kurumizawa H, Tanaka Y and Uzu Y. Solubilization of a water-insoluble dye in aqueous NaBr solutions of alkylpyridinium bromides and its relation to micellar size and shape. *Colloid & Polymer Science*. 2004; 282(3):223-229. http://dx.doi.org/10.1007/s00396-003-0896-z.
25. Wang Y, Chen J, Wei K, Zhang S and Wang X. Surfactant-assisted synthesis of hydroxyapatite particles. *Materials Letters*. 2006; 60(27):3227-3231. http://dx.doi.org/10.1016/j.matlet.2006.02.077.
26. Cullity BD and Stock SR. *Elements of X-ray diffraction*. 3rd ed. New Jersey: Prentice-Hall; 2001.
27. Joris SJ and Amberg CH. Nature of deficiency in nonstoichiometric hydroxyapatites. II. Spectroscopic studies of calcium and strontium hydroxyapatites. *Journal of Physical Chemistry*. 1971; 75(20):3172-3178. http://dx.doi.org/10.1021/j100689a025.
28. Liu JB, Ye XY, Wang H, Zhu MK, Wang B and Yan H. The influence of pH and temperature on the morphology of hydroxyapatite synthesized by hydrothermal method. *Ceramics International*. 2003; 29(6):629-633. http://dx.doi.org/10.1016/S0272-8842(02)00210-9.
29. Blakeslee KC and Condrate RA. Vibrational spectra of hydrothermally prepared hydroxyapatites. *Journal of the American Ceramic Society*. 1971; 54(11):559-563. http://dx.doi.org/10.1111/j.1151-2916.1971.tb12207.x.